NOTICE: When government or other drawings, specifications or other data are used for any purpose other than in connection with a definitely related government procurement operation, the U. S. Government thereby incurs no responsibility, nor any obligation whatsoever; and the fact that the Government may have formulated, furnished, or in any way supplied the said drawings, specifications, or other data is not to be regarded by implication or otherwise as in any manner licensing the holder or any other person or corporation, or conveying any rights or permission to manufacture, use or sell any patented invention that may in any way be related thereto.

ARD-285

SUMMARY REPORT - PHASE II PROGRAM
ANNULAR NOZZLE EJECTOR
CONTRACT NONR 2840(00)

PALO ALTO, CALIFORNIA • CABLE ADDRESS "HILLER" • TELEPHONE DAVENPORT 5-3241

HILLER AIRCRAFT CORP.

In Reply Please Refer to:
ARD-61-M26

July 13, 1961

To: Distribution List

Via: Bureau of Naval Weapons Representative,
Palo Alto, California

Subject: Distribution of Summary Report, Phase II,
Contract Nonr 2840(00), Hiller Report
No. ARD-285

Encl.: (1) Subject Report
(2) Distribution List for Subject Report

1. Subject report is hereby, transmitted to the addressees listed in enclosure (2), per instructions of the Office of Naval Research, Code 461.

2. We would like to hear from you, if this report raises any questions or comments.

HILLER AIRCRAFT CORP.

E. R. Sargent
Manager, Propulsion Dept.
Advanced Research Division

4331/Nonr 2840(00)
GR:gms
Ser 886
19 July 1961

FIRST ENDORSEMENT on HILLER AIRCRAFT CORP ltr ARD-61-M26 of 13 July 1961

From: Bureau of Naval Weapons Representative, Palo Alto, California
To: Distribution List

Subj: Distribution of Summary Report, Phase II, Contract Nonr 2840(00), Hiller Report No. ARD-285

1. Forwarded for information and comment, if appropriate.

G. Robinson
G. ROBINSON

Copy to:
Hiller Aircraft Corp.

DISTRIBUTION LIST

Chief, Bureau of Naval Weapons
Department of the Navy
Washington, 25 D. C.
Attn: Code RAAD-3
Code RR-25
Code R-55

Chief of Naval Operations
Department of the Navy
Washington 25, D. C.
Attn: OP-07T
OP-92

Chief of Naval Research
Department of the Navy
Washington 25, D. C.
Attn: Code 461 (10 copies)
Code 438

Commanding Officer
ONR Branch Office
The John Crerar Library Building
86 East Randolph Street
Chicago 1, Illinois

Commanding Officer
ONR Branch Office
Navy #100, Box #39
Fleet Post Office
New York, New York
Attn: Head, Documents Section
(2 copies)

Commanding Officer
ONR Branch Office
346 Broadway
New York 13, New York

Commanding Officer
ONR Branch Office
1000 Geary Street
San Francisco 9, California

Commanding Officer
ONR Branch Office
495 Summer Street
Boston 10, Massachusetts

Contract Administrator
Southeastern Area
Office of Naval Research
2110 G Street, N. W.
Washington 7, D. C.

Director
Naval Research Laboratory
Technical Information Office
Washington 25, D. C.
(6 copies)

Chief, Bureau of Ships
Department of the Navy
Washington 25, D. C.
Attn: Code 421
Code 529

Commanding Officer and Director
David Taylor Model Basin
Aerodynamics Laboratory
Washington 7, D.C.
Attn: Mr. H. R. Chaplin
(2 copies)

Commanding Officer & Director
David Taylor Model Basin
Hydrodynamics Laboratory
Carderock, Maryland
Attn: Mr. A. Hirsh

Commandant of the Marine Corps
Arlington Annex
Washington 25, D. C.
Attn: Code A04E
Code AAP

Commanding Officer
ONR Branch Office
1030 East Green Street
Pasadena 1, California

Air Force Systems Command
Andrews Air Force Base
Washington 25, D. C.

Aeronautical Systems Division
Wright-Patterson Air Force Base, Ohio
Attn: WWZT, Directorate of Systems Management
WWRPS, Division of Advanced Systems Technology

Office of Chief of Transportation
Department of the Army
Washington 25, D. C.
Attn: TAFO-R

Commanding Officer
U.S. Army Transportation Research Command
Ft. Eustis, Virginia
Attn: TCREC-RDE, Mr. W. Sickles
(2 copies)

Commander
Armed Services Technical Information Agency
Document Service Center
Arlington Hall Station
Arlington 12, Virginia
(10 copies)

Headquarters
National Aeronautics & Space Administration
1512 H Street, N.W.
Washington 25, D. C.
Attn: Mr. Jack Brewer, Code RAA

NASA
Ames Research Center
Moffett Field, California
Attn: Mr. C. W. Harper

Marine Corps Development Center
Marine Corps Schools
Quantico, Virginia
Attn: Air Section

Office, Director of Defense
(Research & Engineering)
Washington 25, D. C.
Attn: Director of Aeronautics

Office of Technical Services
Department of Commerce
Washington 25, D. C.

Cornell University
Graduate School of Aeronautics
Ithaca, New York
Attn: Dr. W. R. Sears

Georgia Institute of Technology
Guggenheim School of Aeronautics
Atlanta, Georgia
Attn: Mr. D. W. Dutton

The Johns Hopkins University
Applied Physics Laboratory
Baltimore 18, Maryland
Attn: Mr. D. W. Rabenhorst

University of Maryland
Institute of Fluid Dynamics & Applied Mathematics
College Park, Maryland
Attn: Prof. Weske
Prof. Shen

Massachusetts Institute of Technology
Aeronautical Engineering Department
Cambridge 30, Massachusetts
Attn: Prof. R. H. Miller

NASA
Langley Research Center
Langley AFB, Virginia
Attn: Mr. R. Kuhn

Mississippi State University
Department of Aerophysics
State College, Mississippi
Attn: Dr. J. J. Cornish

Princeton University
Aeronautical Engineering Department
The James Forrestal Research Center
Princeton, New Jersey
Attn: Mr. T. Sweeney

Stanford University
Guggenheim School of Aeronautics
Palo Alto, California
Attn: Prof. E. G. Reid

Stevens Institute of Technology
Fluid Dynamics Laboratory
Hoboken, New Jersey
Attn: Mr. Peter L. Brown

Syracuse University
Mechanical Engineering Department
Syracuse, New York
Attn: Dr. S. Eskinasi

University of Washington
Department of Aeronautical
Engineering
Seattle 5, Washington
Attn: Prof. F. S. Eastman

University of Wichita
Department of Engineering Research
Wichita 14, Kansas
Attn: Mr. U. Hoehne

A. V. Roe Aeronautical
Group, Ltd.
8921 Sepulveda Blvd.
Los Angeles 45, California
Attn: Mr. W. C. Walter

Aeronutronic
A Division of Ford Motor Co.
Ford Road
Newport Beach, California
Attn: Mr. M. F. Southcote

Aerophysics Corporation
17 Dupont Circle
Washington 6, D. C.
Attn: Dr. G. D. Boehler

AiResearch Manufacturing
Company of Arizona
402 South 36th Street
Phoenix, Arizona
Attn: Mr. L. W. Norman

Armour Research Foundation
3440 South State Street
Chicago 16, Illinois
Attn: Mr. C. C. Miesse

Bell Aircraft Corporation
P. O. Box #1
Buffalo 5, New York
Attn: Mr. H. Mankuta

Bell Helicopter Corporation
P. O. Box 482
Fort Worth 1, Texas
Attn: Mr. R. Lynn

Boeing Airplane Company
Wichita, Kansas
Attn: Mr. H. Higgins

University of Virginia
Aeronautical Engineering Department
Charlottesville, Virginia
Attn: Dr. G. B. Matthews

Chrysler Corporation
Defense Engineering Division
Centerline, Michigan
Attn: Mr. Leonard Hamel

Cleveland Pneumatic Industries, Inc.
Systems Engineering Division
4936 Fairmont Avenue
Bethesda, Maryland
Attn: Mr. William Ellsworth

Collins Radio Company
Cedar Rapids, Iowa
Attn: Dr. A. Lippisch

Convair
Division of General Dynamics Corp.
Mail Zone 6-109
P. O. Box 1950
San Diego 12, California
Attn: Mr. J. E. Loos

Cornell Aeronautical Laboratory, Inc.
4455 Genesee Street
Buffalo 21, New York
Attn: Mr. H. A. Cheilek

Curtiss-Wright Corp.
Wright Aeronautical Div.
Wood-Ridge, New Jersey
Attn: Mr. J. T. Marshall, Jr.

General Atomic
Division of General Dynamics Corp.
P. O. Box 608
San Diego 12, California
Attn: Mr. H. L. Browne

Booz Allen Applied Research, Inc.
4921 Auburn Avenue
Bethesda 14, Maryland
Attn: Mr. W. S. Bull, Jr.

Grumman Aircraft Engineering Corp.
Bethpage, L.I., New York
Attn: Dr. C. E. Mack
Chief of Research

Gyrodyne Corporation of America
Flowerfield
St. James, L.I., New York

Hiller Aircraft Corp.
1350 Willow Road
Palo Alto, California
Attn: Mr. M. F. Gates

Hughes Tool Co.
Aircraft Division
Culver City, California
Attn: M. H. Nay

Hydronautics, Inc.
200 Monroe Street
Rockville, Maryland
Attn: Mr. M. P. Tulin

Library
Institute of the Aeronautical Sciences
2 East 64th Street
New York 21, New York

Lockheed Aircraft Corporation
Burbank, California
Attn: Chief Engineer

Goodyear Aircraft Corp.
Weapons Systems Division
Akron, Ohio
Attn: Mr. J. T. Blair

Lockheed Aircraft Corporation
Georgia Division
86 S. Cobb Drive
Marietta, Georgia
Attn: Dr. J. F. Sutton

Martin Company
Mail Zone A288
Denver, Colorado
Attn: Mr. R. L. Green

Martin Company
Advanced Systems Requirements
Orlando, Florida
Attn: Mr. L. E. Carroll

National Research Associates
P.O. Box #115
College Park, Maryland
Attn: Mr. E. J. Knight

North American Aviation, Inc.
Columbus Division
Columbus 16, Ohio
Attn: P. M. Laub

Piasecki Aircraft Corporation
Island Road
International Airport
Philadelphia 42, Pennsylvannia
Attn: Chief Engineer

Ryan Aeronautical Company
Lindberg Field
San Diego 12, California
Attn: Mr. D. L. Martin

Solar Aircraft
2200 Pacific Highway
San Diego 12, California

Douglas Aircraft Company, Inc.
El Segundo Division
El Segundo, Dalifornia

Therm Advanced Research
Therm, Incorporated
Ithaca, New York
Attn: Dr. A. Ritter

United Aircraft Corporation
Research Laboratories
East Hartford, Conn.
Attn: Mr. L. S. Billman

Vehicle Research Corporation
1661 Lombardy Road
Pasadena, California
Attn: Dr. S. Rethorst

Vertol Aircraft Corporation
Woodland Avenue
Morton Pennsylvannia
Attn: Mr. Stepniewski

California Institute of Technology
Aeronautics Department
Pasadena, California
Attn: Dr. Clark Millikan

Mr. N. K. Walker
7240 Wisconsin Avenue
Bethesda 14, Maryland

Report No. ARD-285

February 1961

SUMMARY REPORT - PHASE II PROGRAM
ANNULAR NOZZLE EJECTOR - CONTRACT NONR 2840(00)

M. F. Gates
Principal Investigator

C. L. Cochran
Research Assistant

Advanced Research
Division of Hiller Aircraft Corp.

1.0 SUMMARY

This report describes the work performed on the Phase II program for Contract Nonr 2840(00) - Annular Nozzle Ejector.

The Phase II program fabricated the full scale ejector assembly and associated equipment. Tests conducted with this hardware indicated that its augmentation performance was approximately 5 points less than that of the small scale hardware ($\phi_{model} = 1.53$, $\phi_{full\ scale} = 1.48$). The jet wake data in combination with jet area distribution indicated the discrepancy between full scale and small scale results may have been caused by less effective ejector action due to the non-uniform momentum curtain. The ejector wake data indicates roughly an order of magnitude reduction in wake wotal pressure and temperature from the unaugmented turbojet.

Ground effect tests were conducted with the small scale model constructed in Phase I. This model geometrically represents the full scale hardware. These tests indicated that an augmentation reduction of approximately 15 points could be anticipated at a ground clearance of 0.35 diameters. The decrease in performance began at approximately 1.3 diameters. Blockage of the secondary flow passages improved performance only below 0.10 diameters ground clearance. Above that level the best performance was obtained by permitting secondary pumping to continue.

TABLE OF CONTENTS

ACKNOWLEDGEMENTS

This study was sponsored by the Office of Naval Research, United States Navy.

The authors also wish to acknowledge the help and guidance afforded by E. R. Sargent, Manager, Propulsion Department and F. A. Heileman, Director, Advanced Research, in the performance of this program. They also wish to thank D. Graber for his interest and invaluable assistance in the test phase, H. Wichers for his photographic coverage and W. Churchill, for his editorial assistance.

FIGURE LIST

SYMBOL LIST

Consistent units are used where required and are otherwise noted.

A_A = Mixing tube throat area

A_e = Mixing tube exit area

A_j = Primary jet exit area

A_s = Bellmouth exit area

A = Area

AR = Aspect ratio = $\left(\frac{\text{Mean Primary Nozzle Circumference}}{\text{nozzle width}}\right)$

C = Discharge coefficient

C_p = Specific heat at constant pressure at operating temperatures

F_m = Measured thrust

g = Gravitational constant

P = Pressure

T = Temperature

V = Velocity

$\dot{w}_m$ = Measured weight flow

J = 778 ft.lb./BTU

γ = Ratio of specific heat at operating temperature

ϕ = Augmentation ratio

ρ = Gas density

As = Entropy change

Subscript

- numerical subscripts see Figure 8

o = Ambient

t = Total

2.0 INTRODUCTION

The Phase I final report presented model test data curves covering the ejector geometry employed in the full scale ejector with the exception of the upstream ducting and plenum chamber. This data for a model which incorporates an extremely high volume, low loss plenum chamber is reproduced in Figure 1.*

The significant ratios of the ejector model which was scaled up for this program were: a mixing-tube-throat to primary-nozzle-throat area ratio, $\frac{A_A}{A_j}$, of 9.74, a mixing tube area ratio, $\frac{A_e}{A_A}$, of 1.95, a mixing-tube-length to throat-diameter ratio of 3, and a primary nozzle aspect ratio, AR, of approximately 100. To reduce costs, a simple, constant area plenum was designed for use with the full scale ejector assembly. In order that model test data be available for intelligent comparison with the full scale data, the model was modified accordingly. Tests of this modification in the first phase program indicated that an augmentation ratio penalty of 5-7 points would occur. This is based on supply total pressure to model, not total pressure at the nozzle exit. It is to be emphasized that for an aircraft installation proper plenum design would essentially eliminate this penalty.

In Phase I of this program the thrust augmentation was referred to the measured thrust of the primary annular nozzle alone corrected

---

*A plotting error previously published in Reference 1 has been corrected and the augmentation reference has also been revised as described in the text.

for secondary flow affects (Reference 1 Appendix). The resulting reference primary thrust is equivalent to that used by other ejector investigators. However, its use in this program has resulted in misunderstandings. Consequently, and henceforth, the thrust augmentation ratio, $\emptyset$, will be referred to the isentropic thrust which would result from expanding the measured primary flow rate adiabatically from the supply total pressure and temperature to ambient pressure. Applying this augmentation reference to the Phase I work would reduce the published augmentation ratios approximately 1%.

3.0 DISCUSSION

A very large portion of the Phase II program was expended in the fabrication of the full scale ejector hardware, thrust table, test installation and necessary instrumentation. Figure 2 shows the complete test installation. Figures 3 and 4 show the details of the ejector primary nozzle and mixing tube, respectively. Appropriate test stand calibration tests and ejector performance evaluation tests were conducted.

This phase also included the evaluation of this same ejector geometry in ground effect using the small scale model fabricated in the first phase program. The same test installation as used in the first phase was used in this work (Refer to Reference 1 Appendix). The linear scale between these two ejectors is approximately 1/9: the thrust scale is approximately 1/86.

The size of the full scale hardware was such as to require only 1/3 of the hot gas output of the J34-WE-36 turbojet; the remainder was bypassed vertically to eliminate any extraneous thrust from the measurements.

3.1 Full Scale Ejector Program

3.1.1 Instrumentation

The instrumentation used in the full scale program was designed to provide a comparison with performance obtained in the previous small scale programs. Factors measured were primary weight flow, total supply pressure, temperature and thrust. The target accuracy was that

established for standard turbojet acceptance tests: ± 1% on thrust and ± 1.5% on airflow rate. Additional instrumentation was used to define both the primary jet total pressure profile and the ejector assembly wake total pressure and temperature profile.

The necessary pressures were measured with appropriate indicators: water manometers for low pressures and mercury manometers for intermediate pressures. The gas temperatures were measured with chromel-alumel thermocouples; the indicating instruments were a Rubicon potentiometer and a self-balancing potentiometer. The thrust was measured on two axes using Hagan "Thrustorq", pneumatic, null balance, load cells. The output of these units was read on bourdon tube "precision test gages" and recorded with a multi-channel Foxboro circular chart recorder.

Figure 5 shows the general arrangement of the load cells in a schematic plan view. Two load cells, one on either side of the ejector centerline, were used to measure the thrust of the complete ejector assembly and/or primary nozzle alone. Figure 6 shows the outboard load cell from the front and its relation to the ejector hardware. The use of two load cells to measure ejector thrust results in the most direct force path. One load cell was used to react the thrust at right angles to the ejector axis (See Figure 7).

Measurement of the primary flow in this full scale system presented something of a problem. Since approximately two-thirds of the jet engine flow was by-passed, it was not possible to calibrate the

engine inlet shroud for flow measurement. Economic considerations precluded using sufficient length of straight, unobstructed duct upstream and downstream of the orifice to meet ASME standards. In addition, the small difference between the turbojet exhaust total pressure and the required supply total pressure to the annular ejector assembly precluded the use of a conventionally sized orifice. The resulting flow section (Fig. 8) incorporated a settling length of 3.1 diameters downstream of the bypass stack, followed by a 1.1 diameters long straightening section. The length-diameter ratio of straighteners was 10 (Fig. 9). This, in turn, was followed by a sharp edged orifice 1 diameter downstream from the straightener section. The diameter ratio of the orifice was approximately 0.84, in order to keep pressure losses low. The sharp edge of the orifice plate was flash chrome-plated to protect it from corrosive effects of hot exhaust gases.

The static pressures were measured approximately 0.76 diameters upstream of this orifice (P_1) and at approximately 0.3 diameters downstream (P_3). At each location four pressure taps were equally spaced around the duct. These were manifolded at each location and connected to the necessary indicating manometers. Downstream from the orifice approximately 0.75 diameters a total pressure and temperature rake was installed to determine the supply conditions at the ejector assembly inlet, (Fig. 10). It is believed that temperature losses between the flow measuring orifice, the measurement point, station 4, and the primary nozzle outlet were insignificant, due to the close coupling of the elements.

3.1.2 Calibration

3.1.2.1 Flow Section

The flow section utilized in this test does not meet ASME standards, consequently, published orifice coefficient data could not be used and calibration was required. The calibrating standard was a 13° half angle, conical nozzle which is shown installed in Figure 11 at the ejector assembly mating flange. The performance of this type nozzle is well documented in Reference 2, which defines the discharge coefficient and velocity coefficient in terms of the pressure and area ratios.

To accomplish the calibration, tests were made at the required supply total pressure (P_{4t}). This was recorded as were the supply total temperature, (T_{4t}), flow orifice (sharp edge) pressure differential ($\Delta P = P_1 - P_3$), static pressure upstream of flow orifice (P_1) and conical nozzle exit area. In addition, the thrust produced by the calibrating conical nozzle was measured. These runs were made for a series of increasing conical nozzle exit areas in order to define the dependence of the flow orifice, flow coefficient ($\dot{K}'$) on jet exit area and pressure differential. With knowledge of the supply conditions (P_{4t} and T_{4t}), and the data of Reference 2, it was possible to determine the test flow rate ($\dot{w}$) and thrust. This flow rate was, in turn, used to determine the flow coefficient, K'.

The compressible flow rate through a conventional orifice

may be determined from $\dot{w} = YA_2K\sqrt{\frac{\Delta P P_1}{T_1}}\left(g\sqrt{2\rho_o\frac{T_o}{P_o}}\right)$ using published data for Y = the conventional expansion factor

and K = standard flow coefficient = $\frac{C}{\left[1-\left(\frac{A_2}{A_1}\right)\right]^{1/2}}$

In this report the flow coefficient is modified to

$$K' = YA_2K\left(g\sqrt{2\rho_o\frac{T_o}{P_o}}\right)$$

and is determined from

$$K' = \dot{w}_m\sqrt{\Delta P\frac{P_1}{T_1}}\Bigg|_{\text{calibration runs}}$$

The resulting calibration curve permits selection of the appropriate value of the flow coefficient (K') for reduction of the ejector performance data. The resulting spread of the K' values was less than 1% of K'. It is believed that the ejector primary flow rate is accurate within a tolerance of ± 1.5%.

The calibration was checked by comparing the measured thrust of the conical nozzle with that computed by use of the data from Reference 2. These values of thrust agree within the limits of accuracy of the referred data.

3.1.2.2 Thrust Calibration

The calibrating elements were Dillon dynamometers of appropriate range which were carefully calibrated on a Tinius Olson

tensile testing machine immediately before use to insure greatest possible accuracy.

3.1.2.2.1 Engine Axis

The calibrating load was applied directly to the thrust table as shown in Figure 12 through the indicating dynamometer by a turnbuckle secured to a "dead-man". The applied load and indicated load (load cell output in psi) were recorded. As expected, the output was found to be linear with applied load. The least squares technique was applied to the data to define the calibration constant. It is believed that the resulting engine thrust data is accurate within ± 1.0%.

3.1.2.2.2 Ejector Axis

Figure 13 shows the setup for thrust calibration along this axis. Indicating dynamometers were installed in both thrust links for this calibration (not visible in the Figure). The calibrating load was applied through a third dynamometer and whiffle tree along the geometrical axis of the ejector assembly by means of a turnbuckle. The data obtained and the resulting calibration were identical to the previous case. Separate calibrations were obtained for each of the two load cells. This permits analysis of differential loading due to misalignment of the thrust axis and the geometrical axis, and thermal expansion. The thrust links are sufficiently long to negate cosine effects enduced by thermal expansion.

3.1.2.3 Over-all Accuracy and Definition of ϕ

The over-all accuracy of the augmentation ratio, ϕ, is ± 3%

where ϕ is defined as follows

$$\phi = \frac{F_m}{\frac{\dot{w}_m}{g} V_{\Delta s=o}},$$

and where

$$V_{\Delta s=o} = \sqrt{2g\ JC_p\ T_{4t}}\ \sqrt{1 - \left(\frac{P_o}{P_{4t}}\right)^{\frac{\gamma-1}{\gamma}}}$$

3.1.3 Results and Evaluation

The prime emphasis of the evaluation tests was to establish the magnitude of Reynold's number and elevated temperature effects on the system performance. Toward this end, tests were made of the primary annular nozzle alone and of the complete annular ejector assembly (including mixing tube). As in the previous model tests, all runs were made at a supply pressure of 21" Hg (pressure ratio of approximately 1.7). The resulting supply temperature was in the 1600-1700°R range. The prescribed pressure was achieved by operating the turbojet at approximately 90% rpm and adjusting the bypass as required. For all runs the equipment was operated for sufficient time to permit equilibrium conditions to be established, as indicated by the total temperature at station 4 (see Figure 8), prior to data recording. The bypass feature permitted much greater flexibility in adjustment of the supply pressure than would have been possible by the conventional throttle alone.

3.1.3.1 Primary Annular Nozzle

The initial series of five tests with the primary nozzle

resulted in an average uncorrected thrust of approximately 1035 pounds. This performance in terms of augmentation ratio, ϕ, is 1.01. The model test results had indicated a comparable primary nozzle performance, ϕ of 0.99. This variance is believed insignificant, particularly when it is considered that the accuracy of ϕ is of the order of ± 3%. During these tests, static pressures measured in the eye of the annulus, as was done in the model tests, indicated slightly greater bellmouth flow for the full scale hardware. This fact tends to support the indicated variance in the primary nozzle performance.

The loss in primary nozzle performance due to the low volume plenum chamber duplicated results of the model tests. This plenum loss amounted to a reduction of approximately 3 points (from a possible ϕ of 1.04 to 1.01).

The primary jet exit was traversed at three locations to determine total pressure profile. These are presented in Figure 14. The average pressure loss indicated by these profiles was approximately 9% (approximately 4% on a thrust augmentation basis). While the variation from point to point is not appreciable, the total effect combined with the area distribution could adversely affect the over-all ejector performance.

In the fabrication of the primary nozzle it was extremely difficult to maintain the concentricity of the inner and outer shells forming the annular nozzle throat. Consequently, the area distribution was non-uniform. In order to reduce the variation below that which existed in the "as spun" and "as assembled" condition, 24 spacers

were incorporated to "equalize" this annular throat as much as possible. It will be noted from the throat dimensions given in Figure 14 that this was not completely successful.

3.1.3.2 Complete Ejector Assembly

Immediately following the evaluation of the primary nozzle, a series of three tests of the complete ejector produced an average uncorrected thrust of 1452 pounds. This performance in terms of augmentation ratio, ϕ, is 1.41 or five points lower than the model test results. The model tests had indicated an augmentation ratio of 1.46 could be achieved with an ejector assembly incorporating the plenum design used in this full scale hardware. Proper plenum design could increase this full scale augmentation performance approximately 7 points to 1.48. This point has been located in Figure 1. It is believed that the loss in performance between the small scale work and the full scale work can be attributed, at least partially, to the non-uniformity of the area distribution discussed in paragraph 3.1.3.1.

The work of Reference 3 points out that scale (Reynold's number) effects are negligible and that the effects of an elevated temperature primary gas are self compensating. The increased temperature at the same supply pressure produces a higher velocity primary jet which decreases the basic mixing efficiency. In contrast, the increased viscosity of the elevated temperature primary jet improves the mixing process. The net effect of temperature is seen to be negligible.

The subsequent test program to substantiate this performance and to determine means of improving it was characterized by

erratic and deteriorating performance. Recalibration of the instrumentation did not reveal the source of difficulty.

Prior to dismantling the assembly for internal inspection the wake was traversed one exit diameter downstream of the mixing tube to determine the wake total pressure and temperature profiles. This data is presented in Figure 15.

Immediately following this test the mixing tube was removed and spot checks of the primary wake total pressure were made. These checks revealed that the average jet pressure loss had increased to approximately 23%, i.e., the effective total pressure for correlation of this exit wake profile data was approximately 17 inches of mercury. It was also noted that the primary performance had deteriorated. This same information pointed out the probable cause of the inferior performance.

Referring again to the wake profiles in Figure 15, it is seen that an appreciable reduction is achieved in the basic jet temperature and pressure. The peak exit pressure is seen to be 17.5 inches of water or approximately 15 fold reduction; the peak temperature is 200°F (660°R), or a 4 fold reduction from the approximate 1620°R jet exit temperature.

3.1.3.3 Primary Annular Nozzle Damage

Inspection of the interior of the duct system, starting with the straightener section revealed no cause for the increase in pressure loss or for erratic performance. Inspection of the primary nozzle inlet revealed that the divider plate (-35 in Figure 3) had been

severely damaged, apparently by thermal fatigue in combination with differential expansion between the duct outer walls and the divider plate. Figure 16 shows the damage to the divider plate which was originally installed to improve the diffusion into the plenum chamber. The right hand photo in Figure 16 shows that a large "tab" (approximately 5 x 7 inches) was torn from the divider prior to this complete failure. Markings on the inner wall of the duct indicate that this "tab" had flexed up and down several times, which probably caused the erratic, poor performance. The complete failure of the divider plate reduced the duct area approximately 80 percent. This undoubtedly was the cause of the high indicated plenum loss. Complete repair of this damage was not possible prior to the end of this phase of the program. This work will be continued into the subsequent phase.

3.2 Small Scale Annular Nozzle Ejector Ground Effect Evaluation

Ejector performance tests were conducted in ground effect, using the small scale hardware which was fabricated in Phase I. This hardware represents the full scale configuration. It should be emphasized that this original configuration was optimumized for out-of-ground effect operation and does not necessarily represent an optimum ground effect configuration. The data is presented in Figure 17 as augmentation ratio versus dimensionless ground clearance. It will be noted that there is a gradual deterioration in performance as the ground clearance is decreased below approximately 1.3 diameters. This deterioration continues to approximately 0.4 diameters ground clearance at which point the augmentation ratio is approximately 1.3. Further reduction of

ground clearance improves ϕ. In fact, at ground clearances less than 0.15 diameters, ϕ is greater than that out-of-ground effect. The reason for this performance is hypothesized as follows: the ground plane became an influence in the cycle by increasing the static pressure at the mixing tube exit plane. At first, this pressure was only sufficient to cause a reduction in the secondary mass flow handled and not sufficient to cause a net gain in performance due to its reaction on the downward facing projected area of the diffusing mixing tube. By continuing to decrease the ground clearance, the exit static pressure increased to the point where a depression no longer existed at the eye and consequently, bellmouth pumping was stopped. This occurred at approximately 0.15 diameters ground clearance. The exit static pressure acting on downward facing projected area of the mixing tube at this ground clearance was sufficient to improve performance. It was found that the mixing tube inlet continued to pump to approximately 0.08 to 0.12 diameters ground clearance.

It will be noted that only below 0.1 diameters ground clearance was any benefit derived from complete blockage of either of the secondary flow paths, the bellmouth or mixing tube inlet.

The problems encountered with the full scale hardware precluded further expenditure of effort in the ground-effect regime.

4.0 CONCLUSIONS

4.1 The effect of the ejector size (Reynolds' number) on ejector performance is negligible.

4.2 The effect of elevated temperature on ejector performance is negligible.

4.3 The maldistribution of jet area and jet total pressure is probably largely responsible for the variation between small and full scale ejector performance.

4.4 A performance penalty can be expected with the present ejector configuration when operating at ground clearance from 1.3 to 0.15 diameters. Below 0.15 diameters superior performance is achieved.

4.5 Roughly an order of magnitude reduction of the wake temperature and total pressure is achieved by the use of the ejector system over a straight turbojet exhaust.

5.0 REFERENCES

1. Spiegelberg, C. H.: "Summary Report - Annular Nozzle Ejector" - Contract Nonr 2840(00), Hiller Aircraft Corp., Advanced Research Division Report No. 243, November 1959.

2. Grey, Ralph E., Jr., and Wilsted, H. Dean: "Performance of Conical Jet Nozzles in Terms of Flow and Velocity Coefficients", NACA Report No. 933.

3. Bertin, J., and Le Nabour, M.: "Contribution Au Développement Des Trompes et Éjecteurs", De La Société Bertin and C^{ie}, Technique et Science Aeronautiques, Tome 3, 1959.

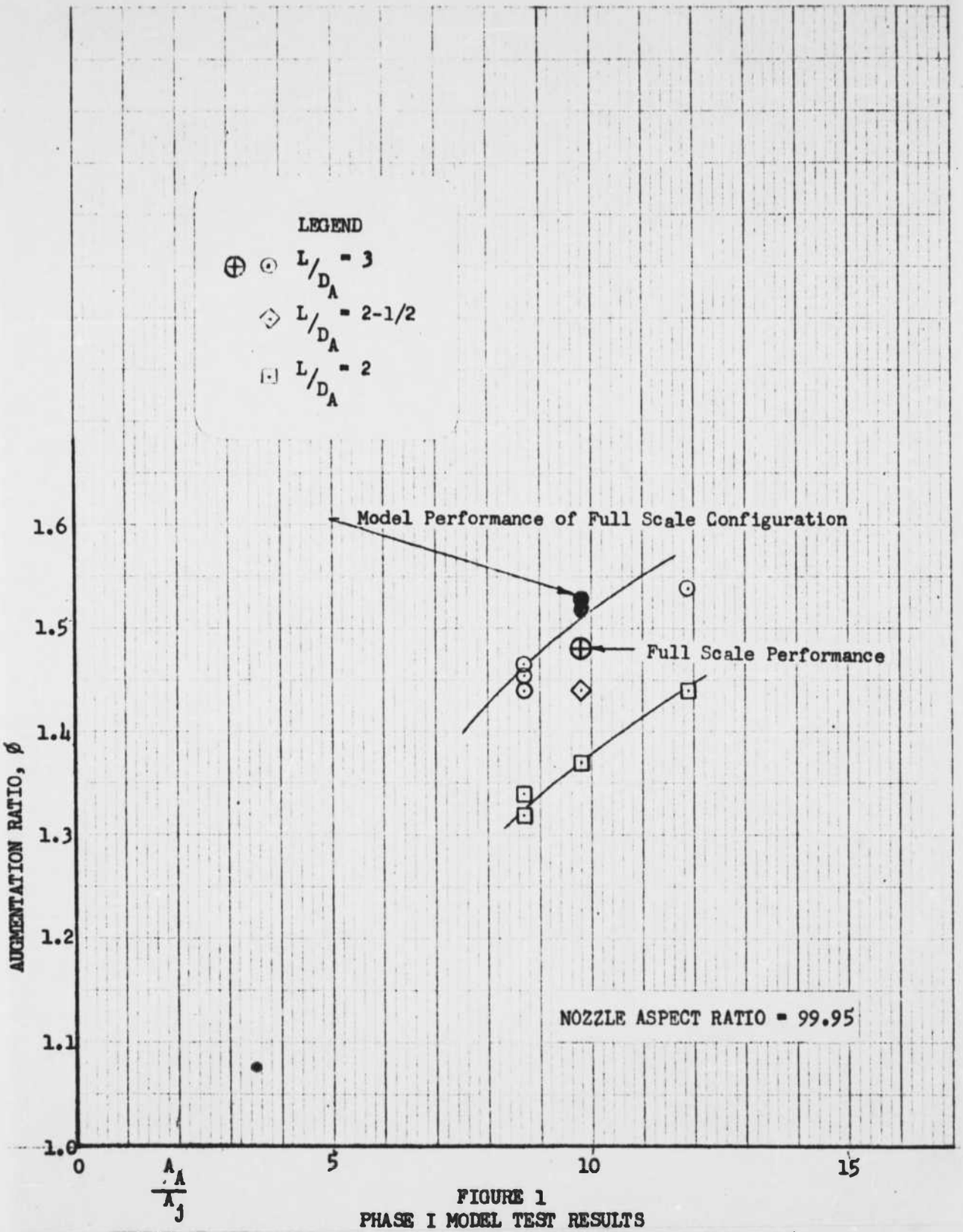

FIGURE 1
PHASE I MODEL TEST RESULTS
EFFECT OF AREA RATIO ON AUGMENTATION PERFORMANCE AT CONSTANT L/D RATIOS
FOR DIFFUSING MIXING TUBES

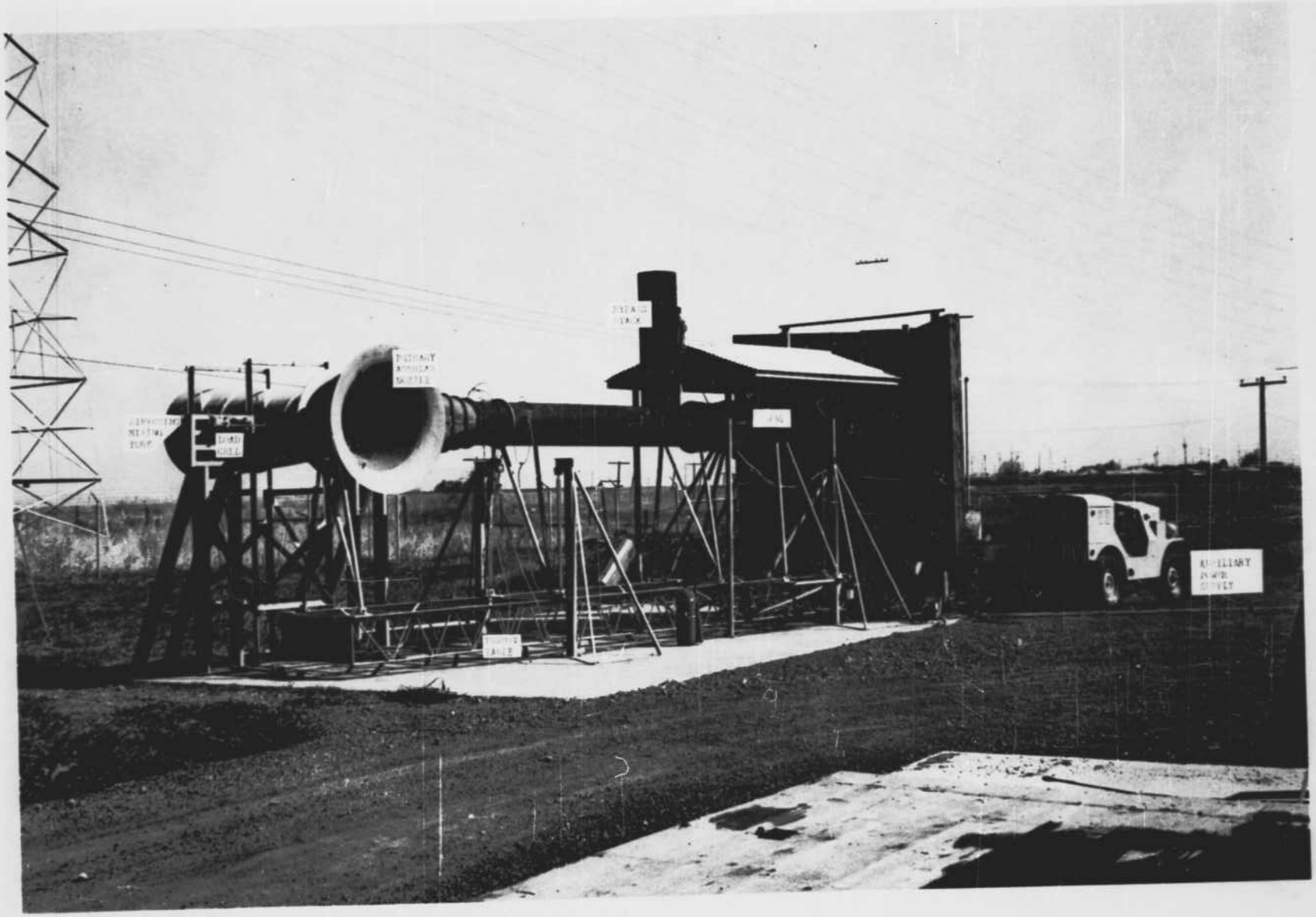

FIGURE 2: COMPLETE EJECTOR ASSEMBLY AND J34 TURBOJET ENGINE TEST INSTALLATION

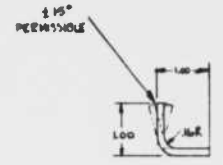

TYPICAL ANGLE SECTION
FOR -17 THRU -29

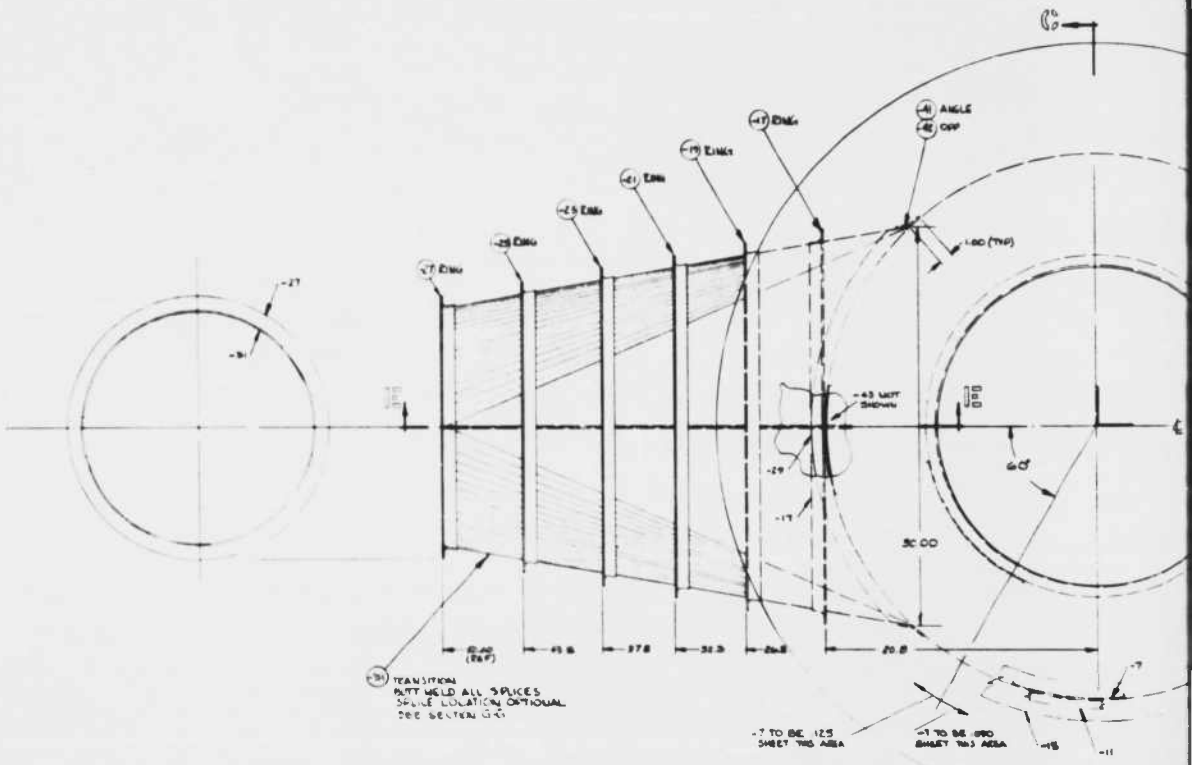

FRONT VIEW

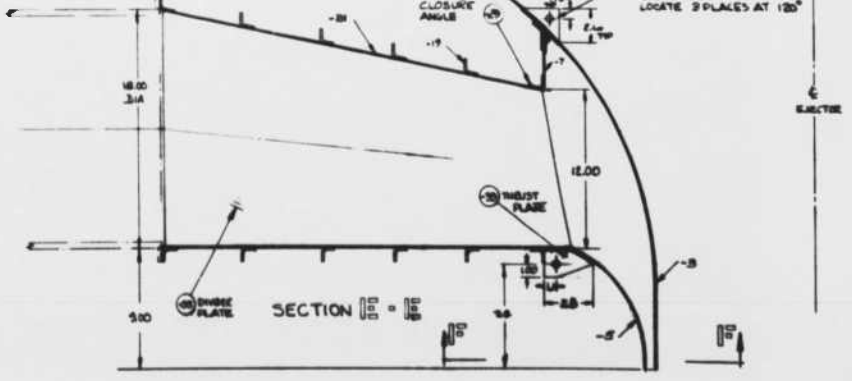

1

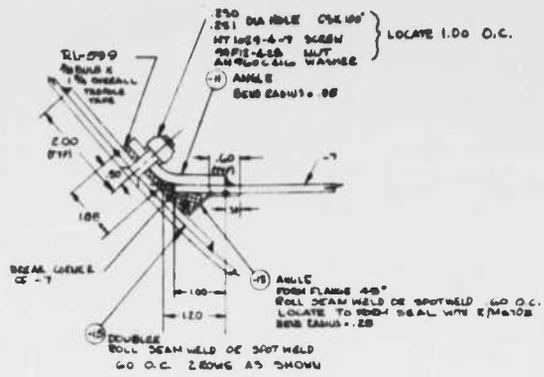

VIEW A

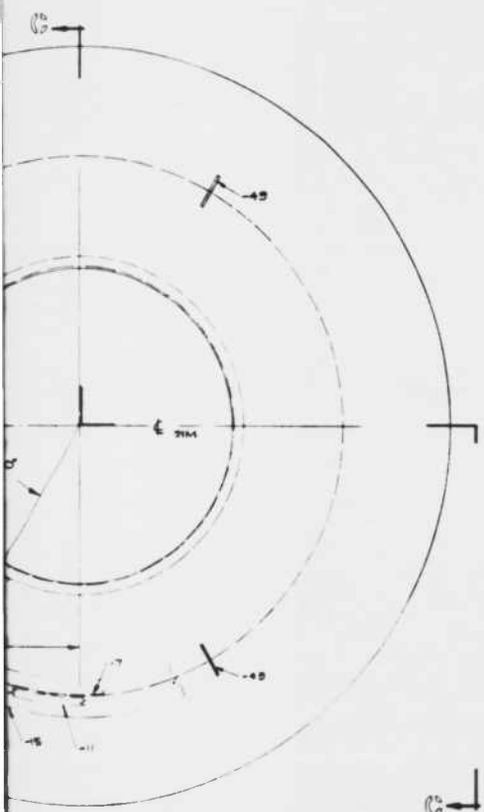

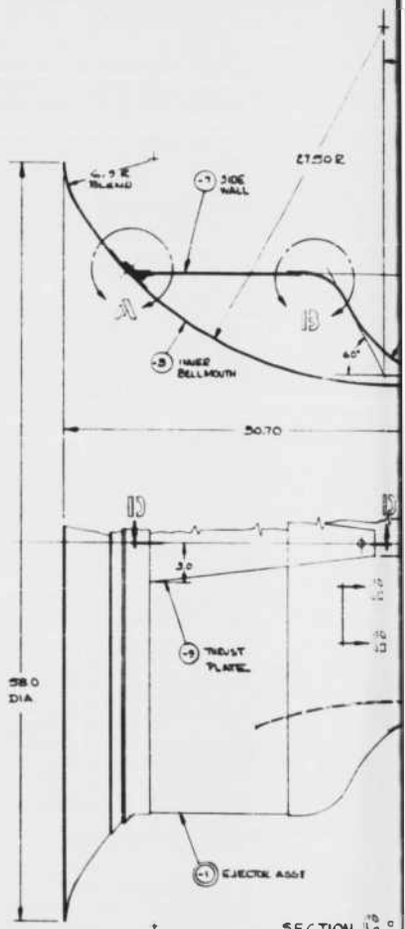

SECTION

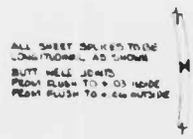

SECTION
TYPICAL FOR -3, -5, -7, -31

POINT VIEW

AT 120°

EJECTOR

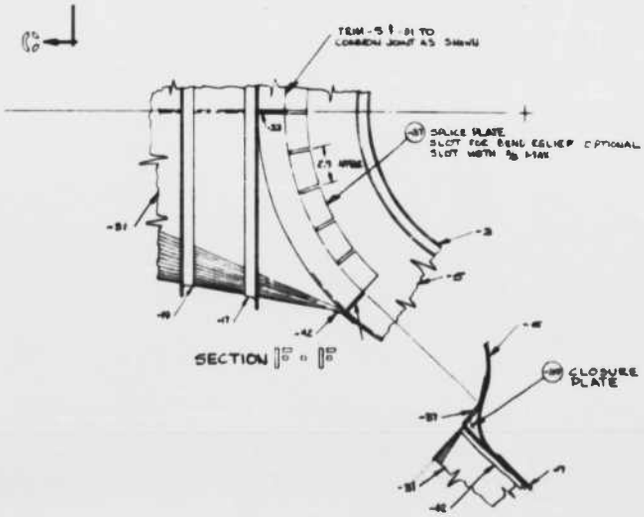

SECTION

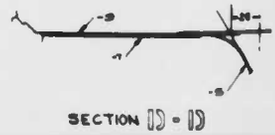

SECTION

2

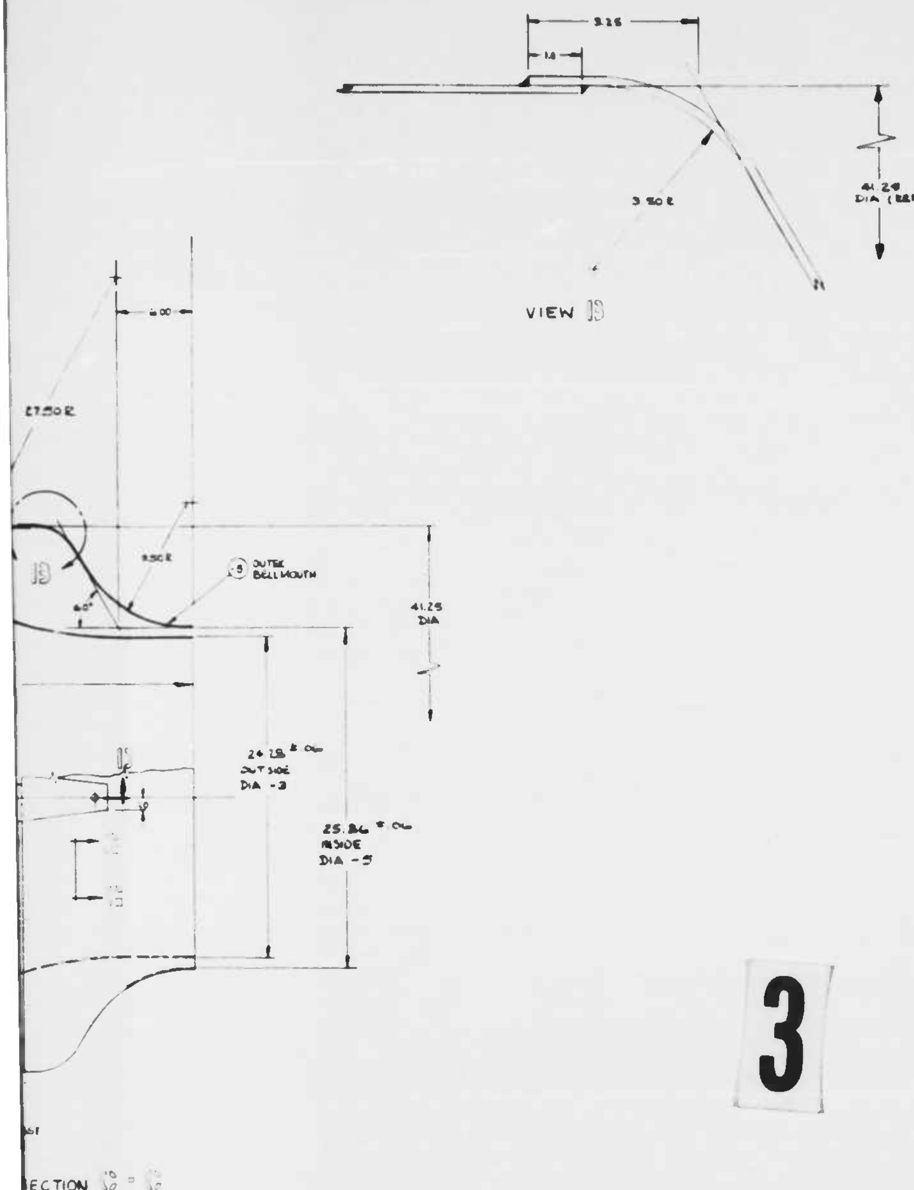

3

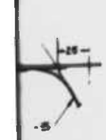

40	NT 1029-4-10	SCREW	VOI-SHAN	CULVER CITY, CAL
40	99F12-4E8	NUT	SPS	
40	AN960C416	WASHER		
6'	RL-599	TEMPOLE TAPE	[illegible]	R/M, PASSAIC, N.J.

Qty	Part No.	Part Name	Thickness	Material
3	-41	LIFTING LUG	.125 SHEET	STAINLESS STEEL ALLOY [illegible]
	-[illegible]	ANGLE	.125	
2	-39	CLOSURE PLATE	.125	
1	-37	[illegible] PLATE	.125	
1	-35	DIVIDER PLATE	.090	
1	-33	THRUST PLATE	.125	
1	-31	TRANSITION	.125	
1	-29	CLOSURE ANGLE	.125	
1	-27	RING	.125	
1	-25		.125	
1	-23		.125	
1	-21		.125	
1	-19		.125	
1	-17	RING	.125	
1	-15	DOUBLER	.090	
1	-13	ANGLE	.082	
1	-11	ANGLE	.125	
1	-9	THRUST PLATE	.125	
1	-7	SIDE WALL	.090 & .125	[illegible] VIEW
1	-5	OUTER BELLMOUTH	.125	
1	-3	INNER BELLMOUTH	.125 SHEET	STAINLESS STEEL ALLOY [illegible]
	-1	EJECTOR ASSY		

2 ALL LIFTING LUGS AND THRUST PLATES TO HAVE ½" DIA. HOLES

3 ASSEMBLE ENDS WITH CONTINUOUS FUSION WELD AROUND LEG OF ANGLE WELD ⅛" x 1" [illegible] AT HEEL OF ANGLE

3 ASSEMBLE TO MATING PART WITH CONTINUOUS FUSION WELD ON BOTH SIDES OF JOINT

4 DYE PENETRANT INSPECT ALL FUSION WELDS

5 BUTT WELD FORMED SECTION AS REQD

6 BUTT WELD SHEET STOCK AS REQD - SEE SECTION G-G

1 THIS ASSEMBLY OPERATES AT JET ENGINE TAILPIPE TEMPERATURE AND PRESSURE. THIS IS APPROXIMATELY 1200°F AND 20 PSIG. FABRICATING TECHNIQUES MUST BE CONSISTENT WITH, AND ALL CONSTRUCTION MUST BE PRESSURE TIGHT FOR, THIS CONDITION

NOTES - UNLESS OTHERWISE SPECIFIED

STRESS RELIEVE AT 1200°F

ANNULAR EJECTOR ASSEMBLY

NONE

HILLER HELICOPTERS PALO ALTO, CALIF.

AR23-1007

FIG 3

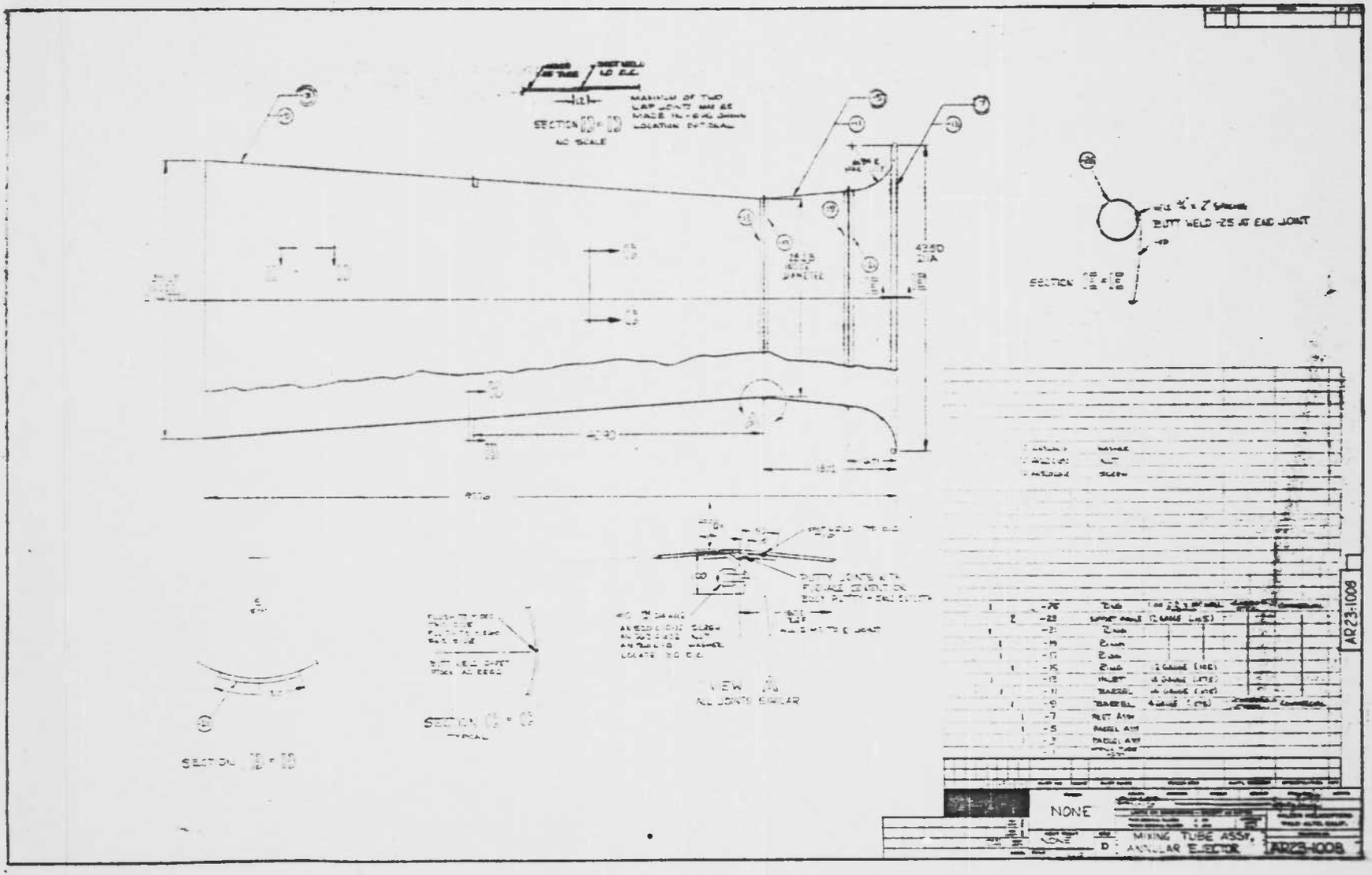

FIGURE 4: MIXING TUBE ASSEMBLY

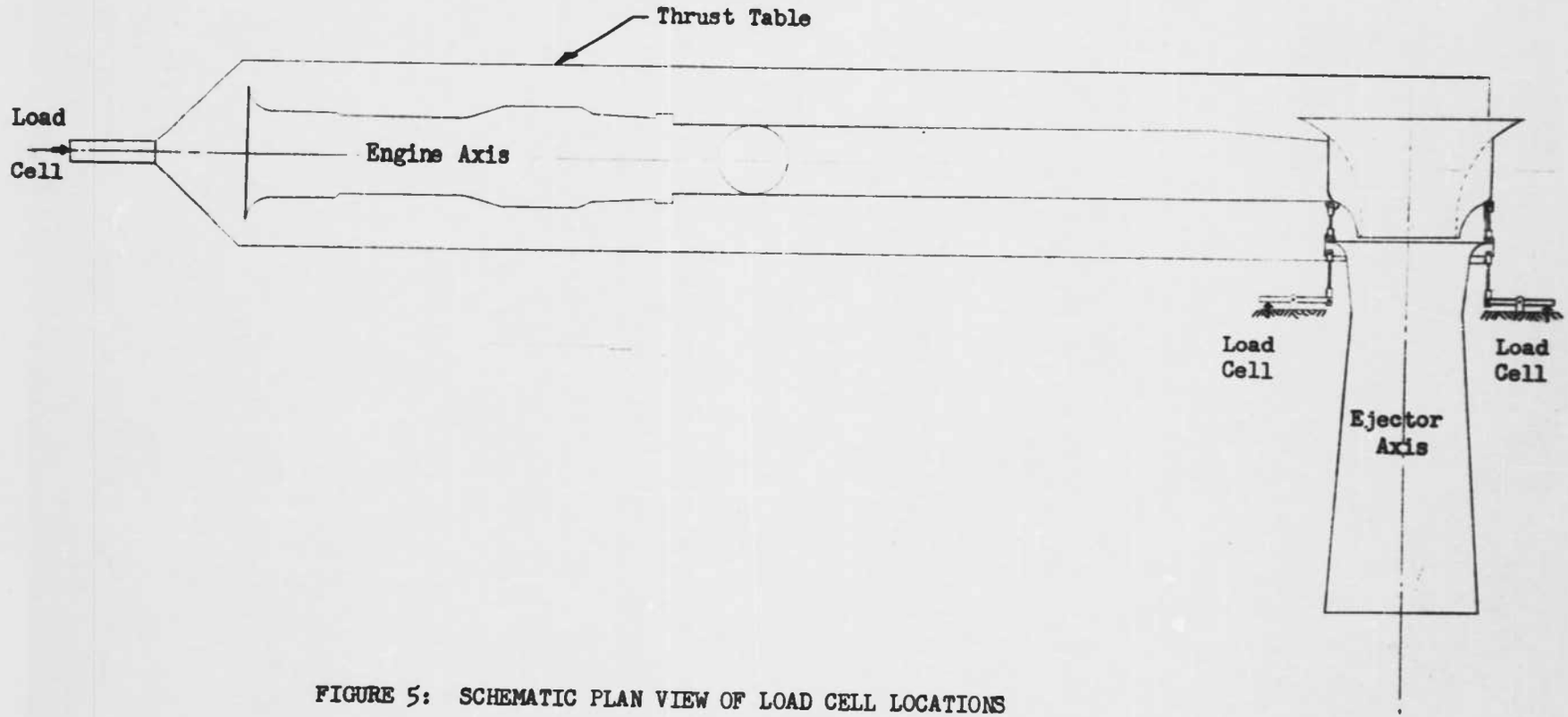

FIGURE 5: SCHEMATIC PLAN VIEW OF LOAD CELL LOCATIONS

FIGURE 6: EJECTOR AXIS LOAD CELL INSTALLATION (FRONT VIEW)

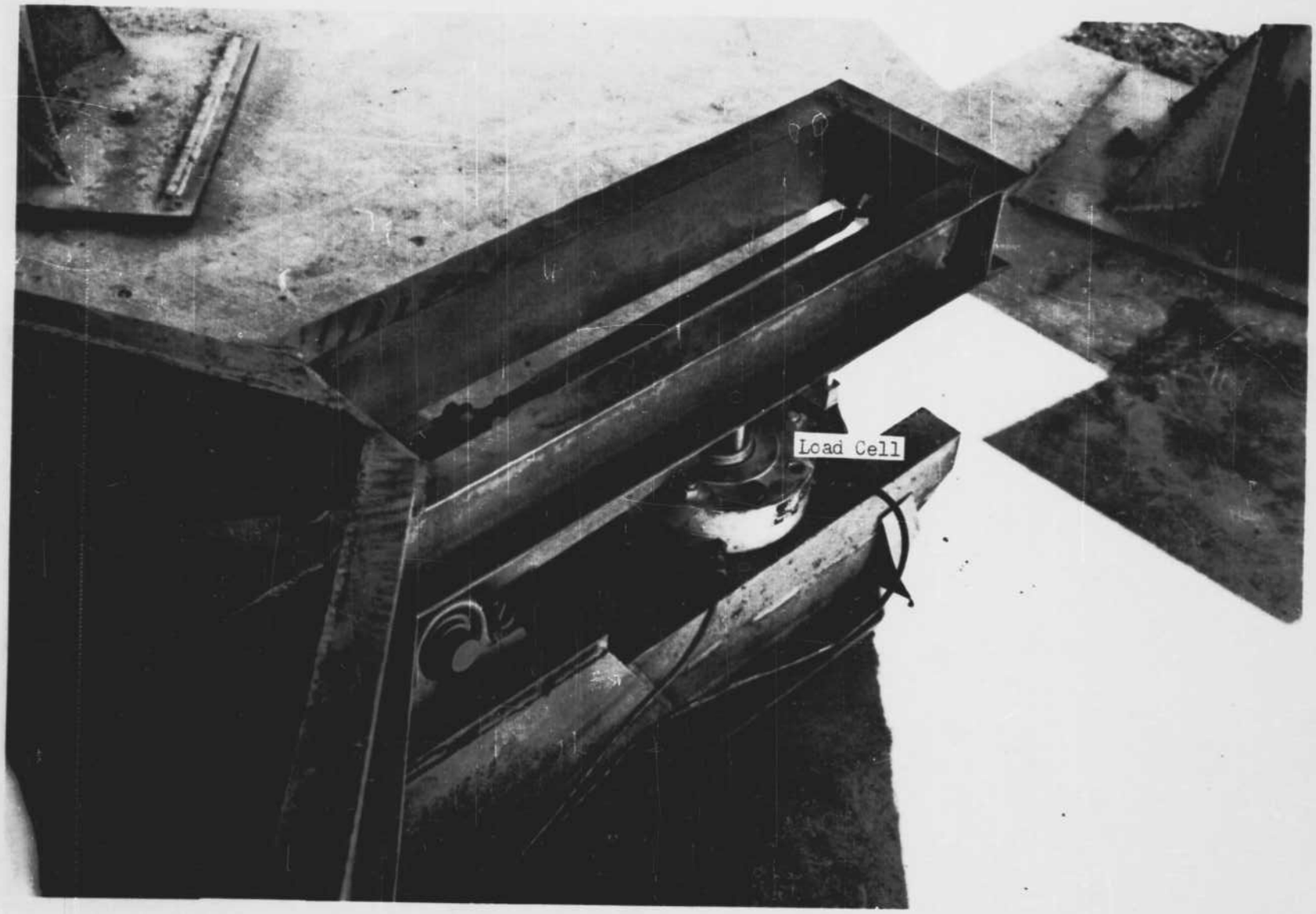

FIGURE 7: ENGINE AXIS LOAD CELL INSTALLATION

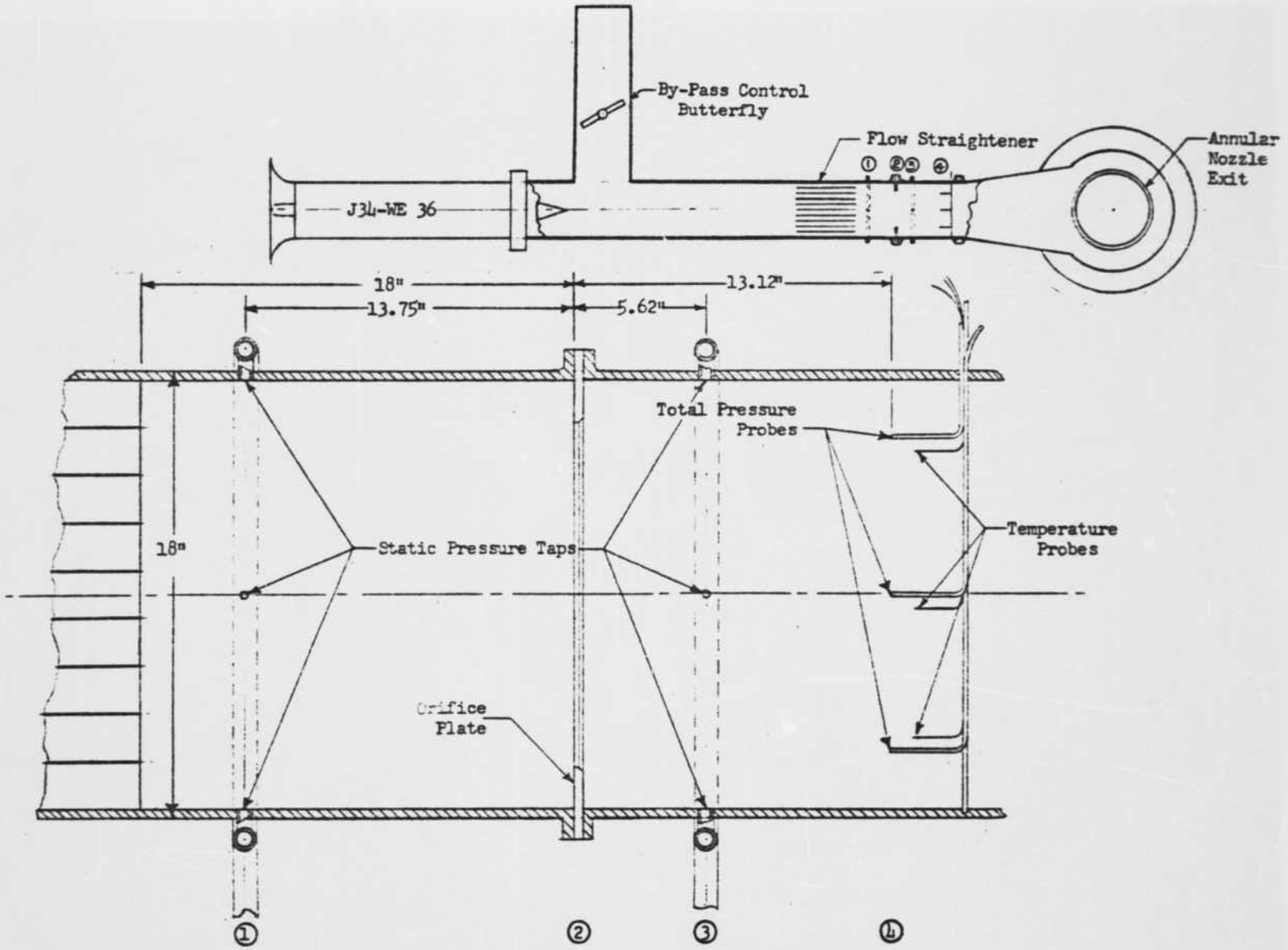

FIGURE 8: FLOW SYSTEM SCHEMATIC

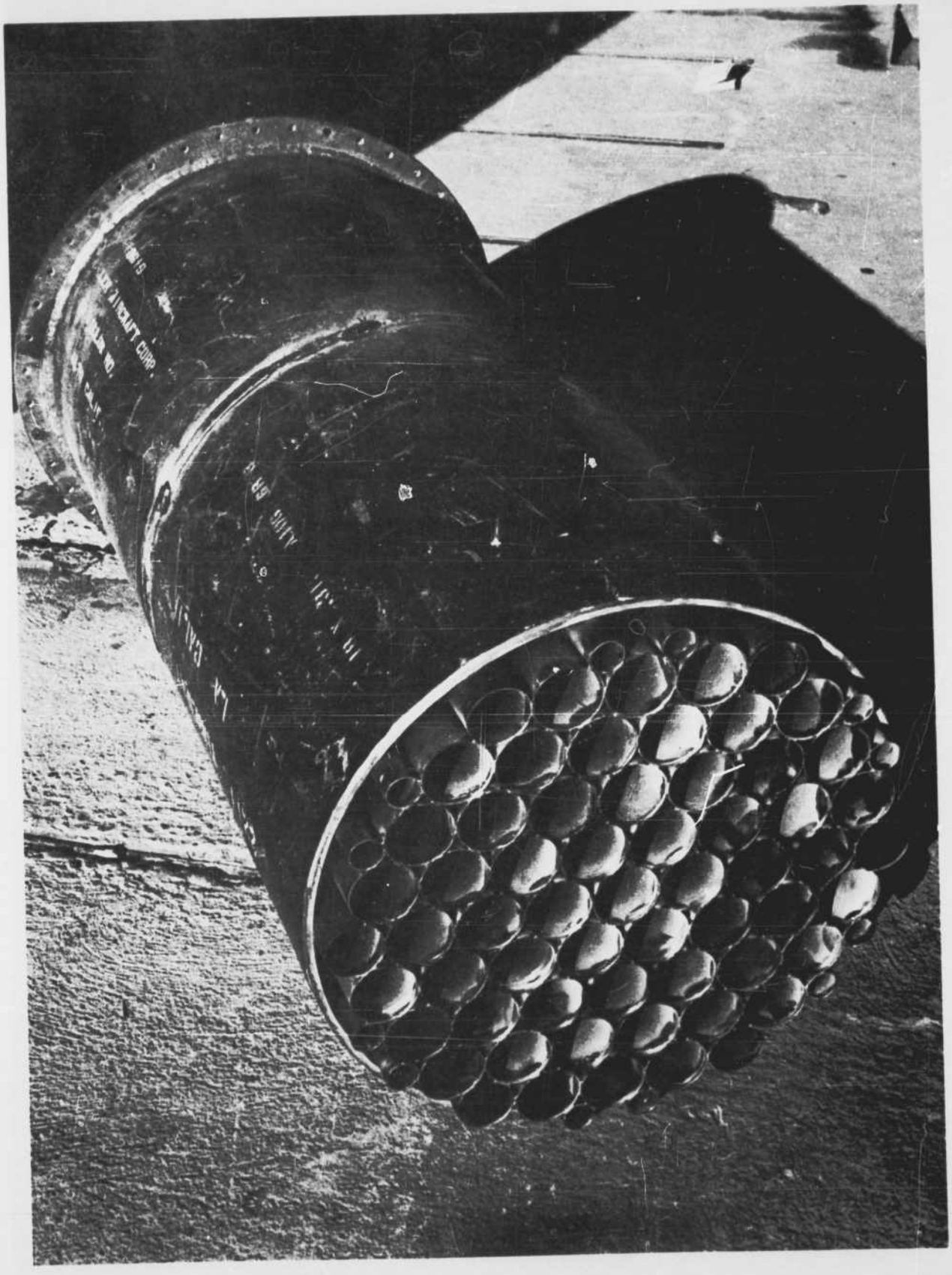

FIGURE 9: FLOW STRAIGHTENER

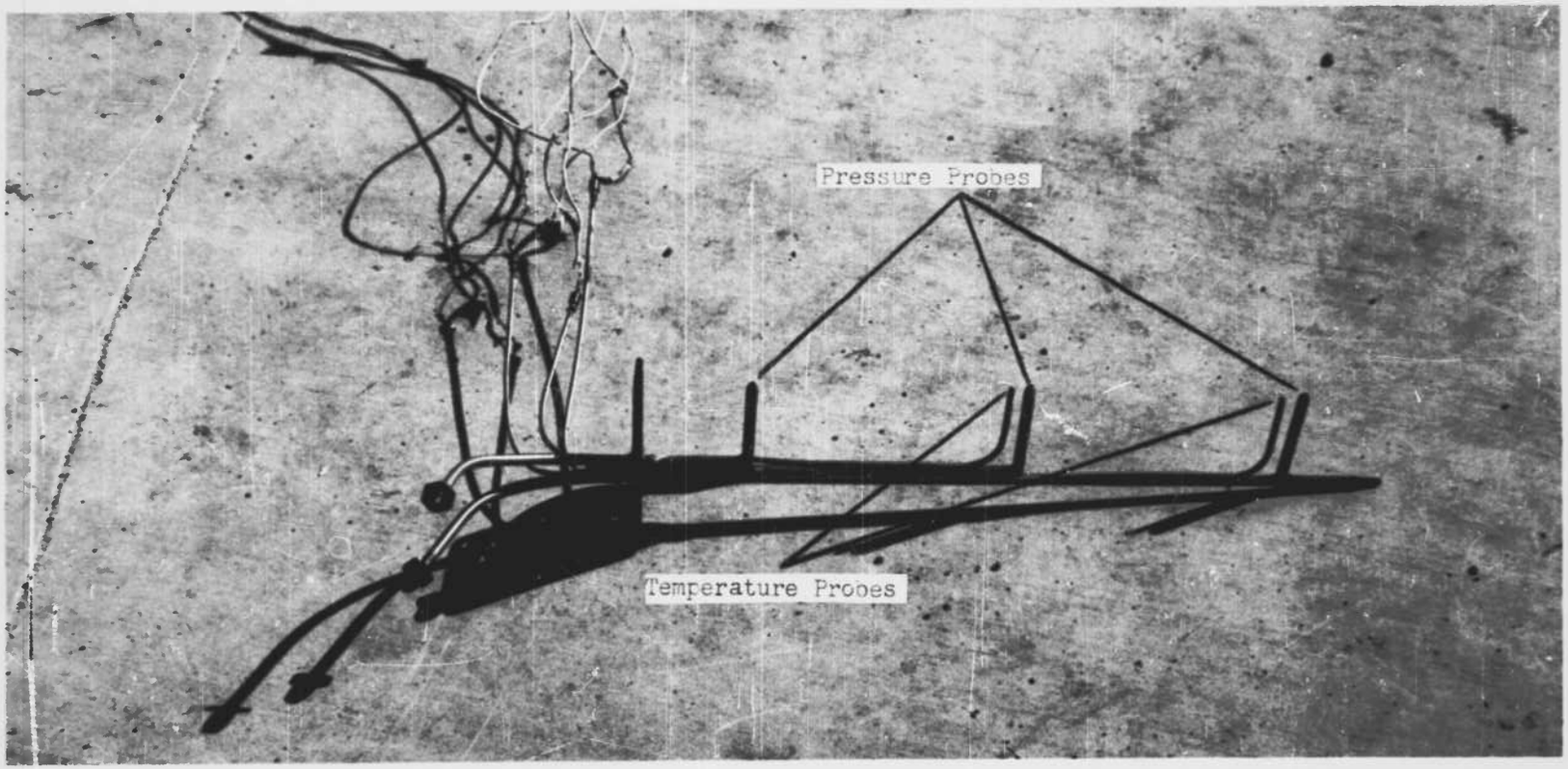

FIGURE 10: TOTAL PRESSURE AND TEMPERATURE RAKE (REF. FIG. 8)

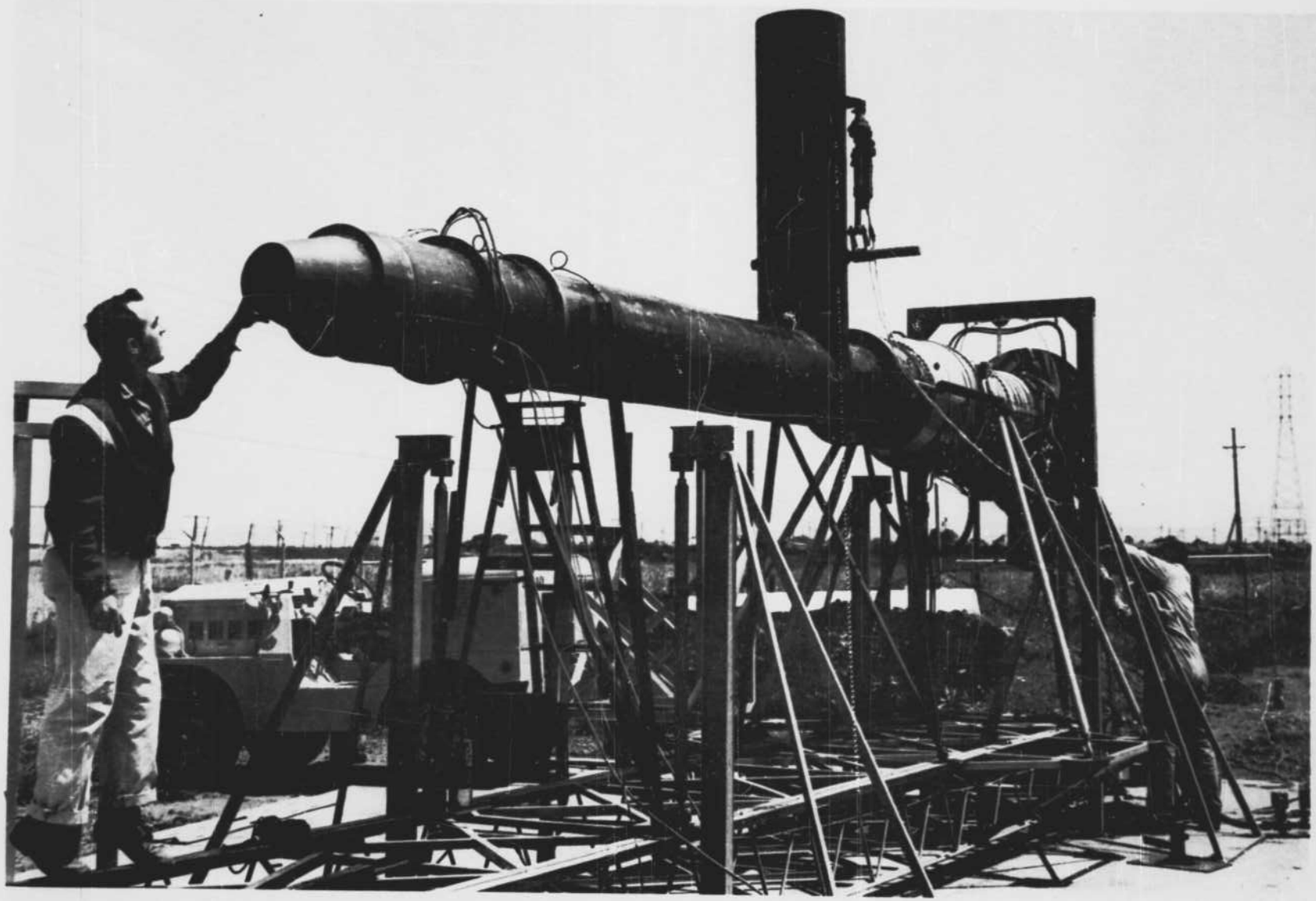

FIGURE 11: FLOW ORIFICE CALIBRATION SET-UP

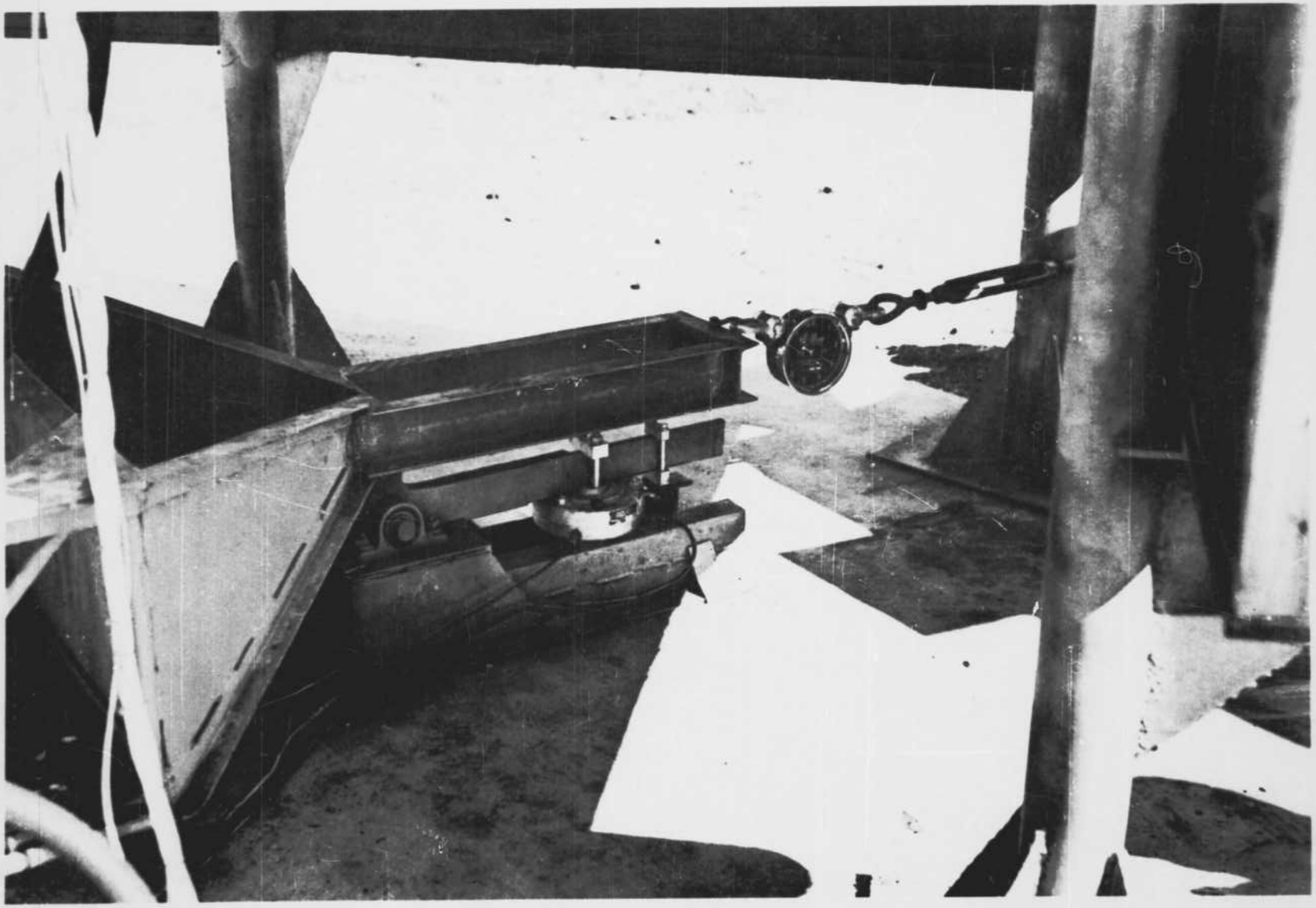

FIGURE 12: ENGINE AXIS LOAD CELL CALIBRATION SET-UP

FIGURE 13: EJECTOR AXIS LOAD CELL CALIBRATION SET-UP

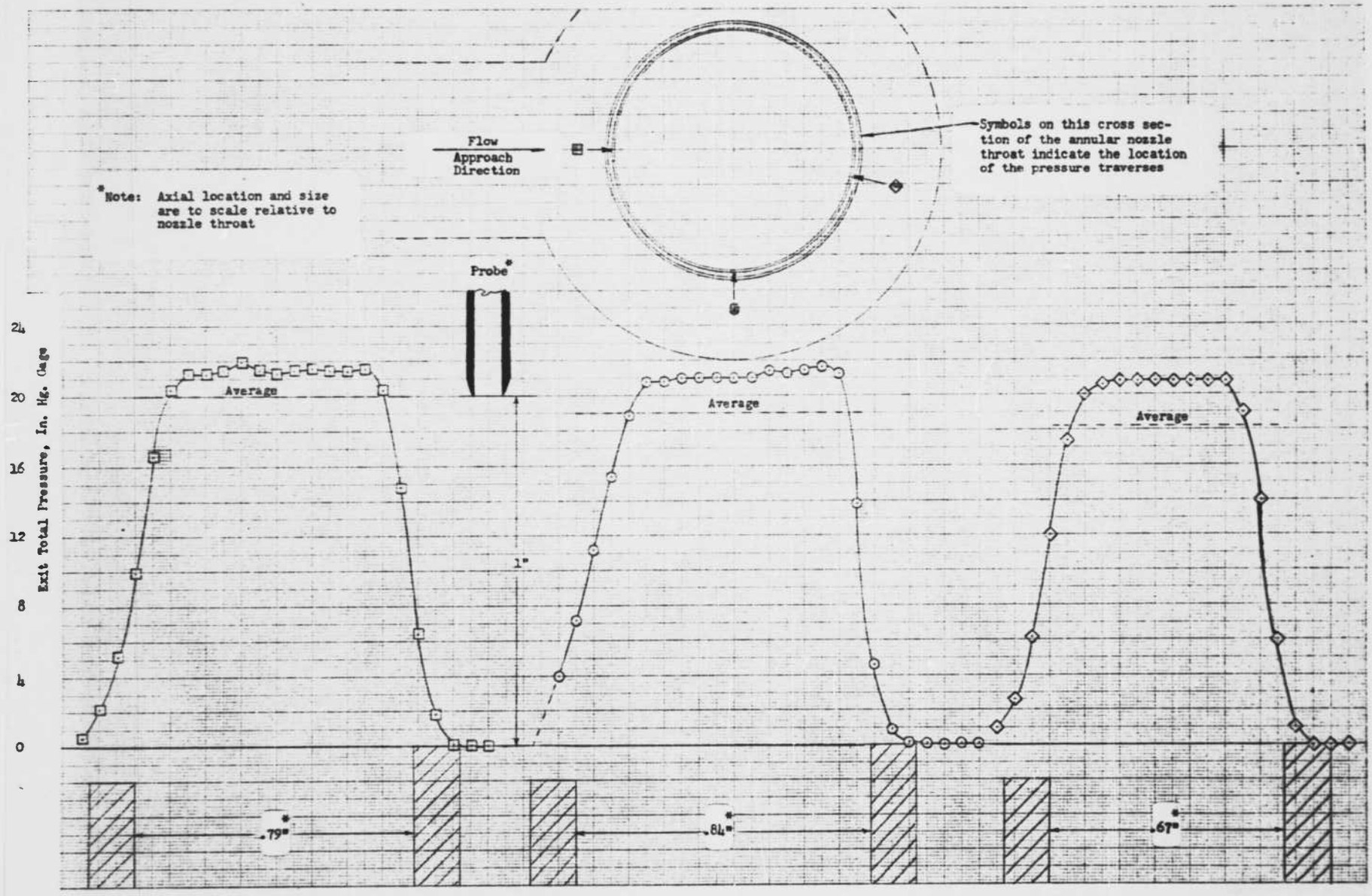

FIGURE 14: PRIMARY JET TOTAL PRESSURE PROFILE

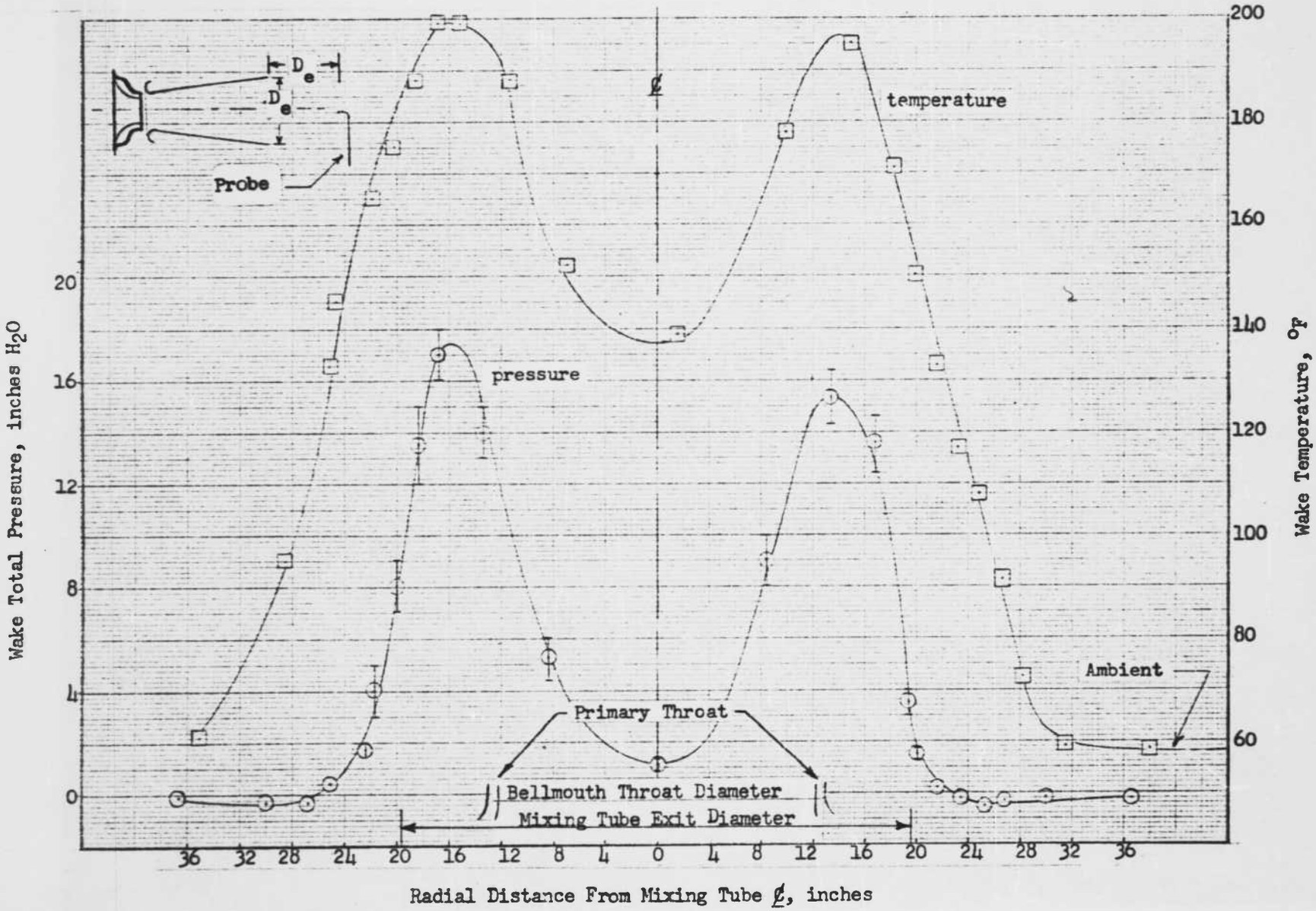

FIGURE 15: WAKE TOTAL PRESSURE AND TEMPERATURE PROFILE - EJECTOR ASSEMBLY

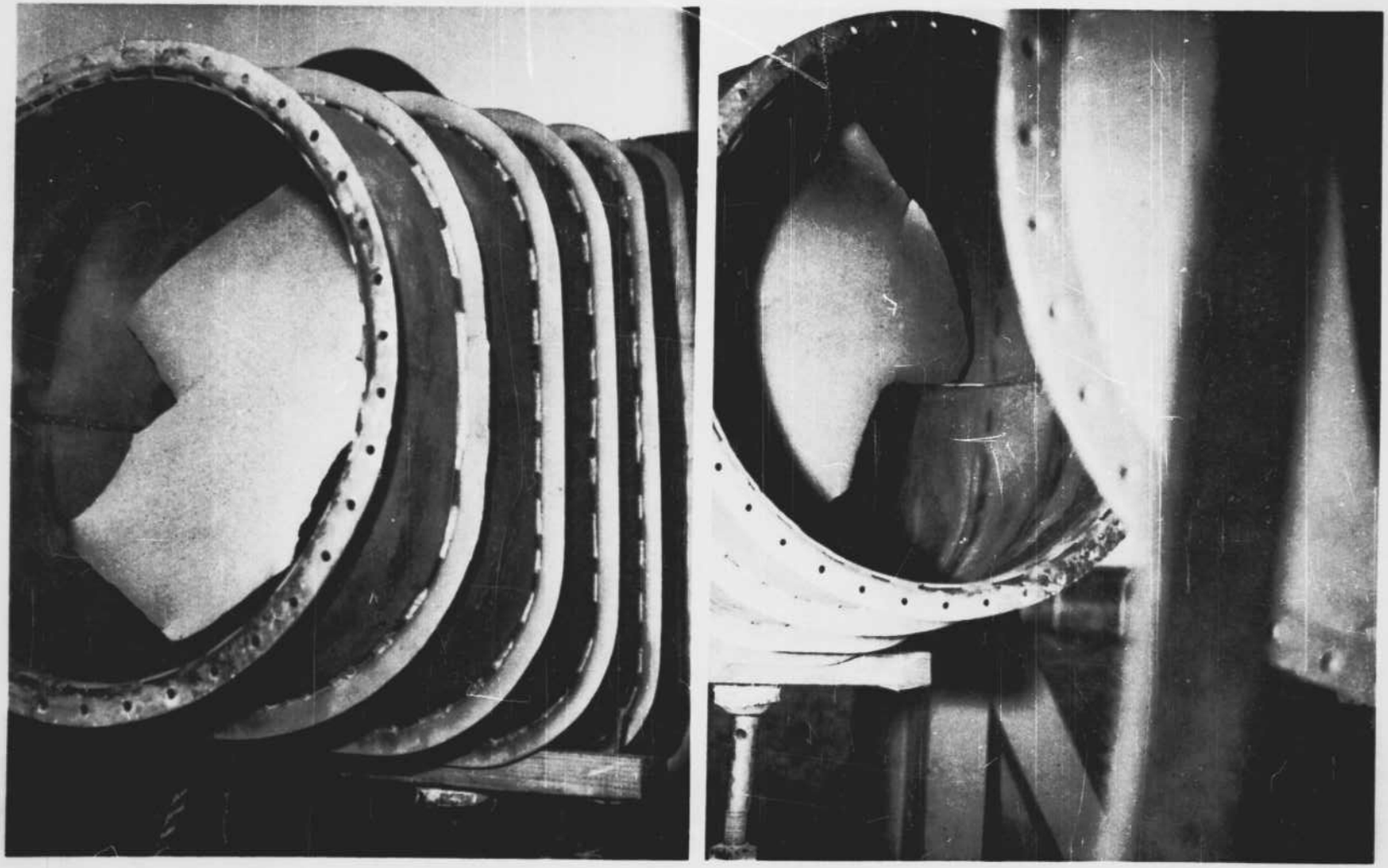

FIGURE 16: DIVIDER PLATE (RIGHT AND LEFT HAND VIEWS)

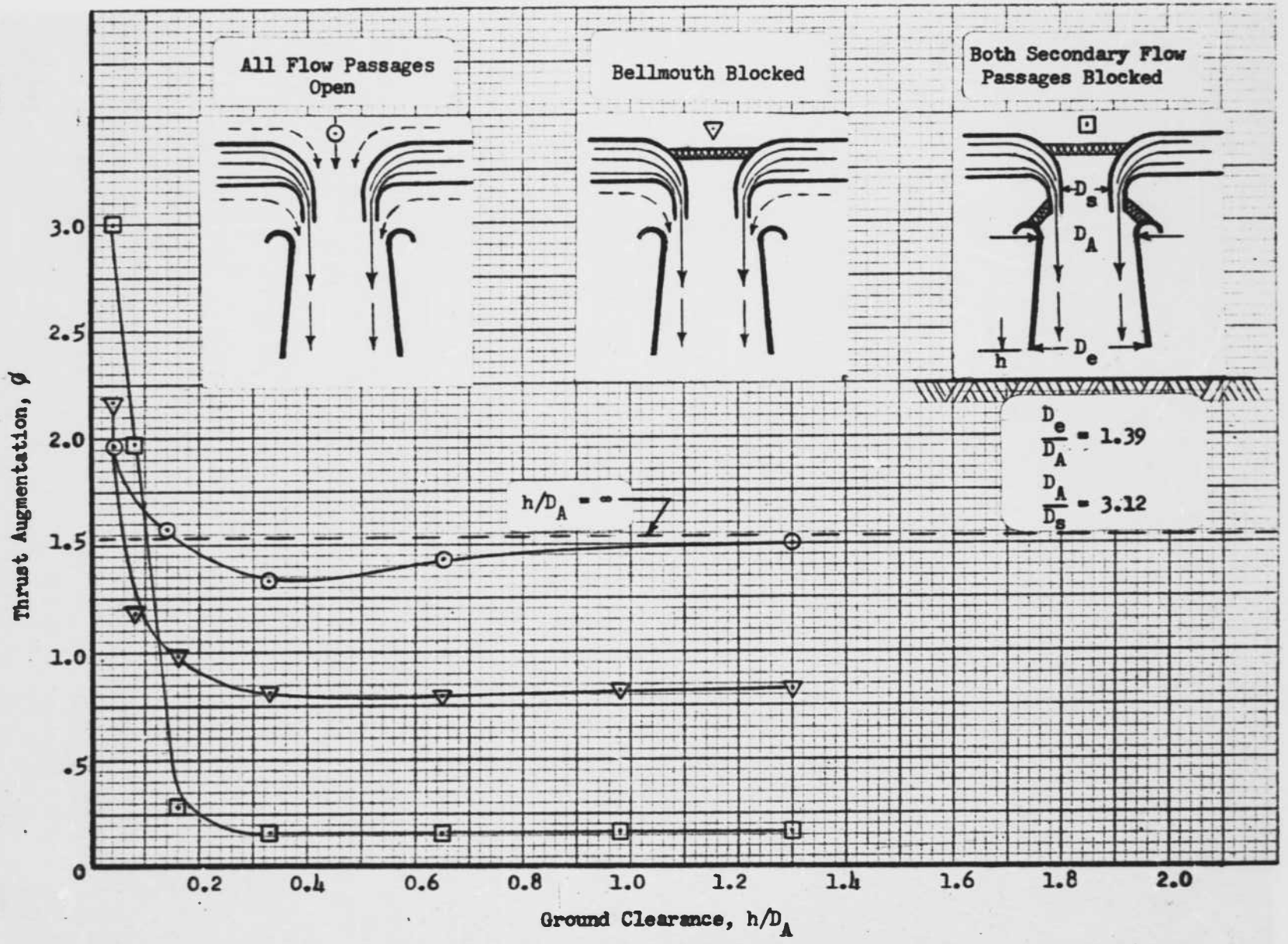

FIGURE 17: GROUND EFFECT PERFORMANCE OF ANNULAR EJECTOR